

Accepted Manuscript

Supramolecular spectral studies on metal-ligand bonding of novel quinoline azodyes

M.A. Diab, A.Z. El-Sonbati, A.A. El-Bindary, A.M. Barakat

PII: S1386-1425(13)00801-9
DOI: <http://dx.doi.org/10.1016/j.saa.2013.07.053>
Reference: SAA 10797

To appear in: *Spectrochimica Acta Part A: Molecular and Biomolecular Spectroscopy*

Received Date: 25 May 2013
Revised Date: 15 July 2013
Accepted Date: 22 July 2013

Please cite this article as: M.A. Diab, A.Z. El-Sonbati, A.A. El-Bindary, A.M. Barakat, Supramolecular spectral studies on metal-ligand bonding of novel quinoline azodyes, *Spectrochimica Acta Part A: Molecular and Biomolecular Spectroscopy* (2013), doi: <http://dx.doi.org/10.1016/j.saa.2013.07.053>

This is a PDF file of an unedited manuscript that has been accepted for publication. As a service to our customers we are providing this early version of the manuscript. The manuscript will undergo copyediting, typesetting, and review of the resulting proof before it is published in its final form. Please note that during the production process errors may be discovered which could affect the content, and all legal disclaimers that apply to the journal pertain.



Supramolecular spectral studies on metal-ligand bonding of novel quinoline azodyes

M.A. Diab, A.Z. El-Sonbati[†], A.A. El-Bindary, A.M. Barakat*
Chemistry Departments, Faculty of Science, Damietta University, Damietta, Egypt

Abstract

A series of novel bidentate azodye quinoline ligands were synthesized with various *p*-aromatic amines like *p*-(OCH₃, CH₃, H, Cl and NO₂). All ligands and their complexes have been characterized on the basis of elemental analysis, IR, ¹H and ¹³C NMR data and spectroscopic studies. IR and ¹H-NMR studies reveal that the ligands (HL_{*n*}) exists in the tautomeric azo/hydrazo form in both states with intramolecular hydrogen bonding. The ligands obtained contain N=N and phenolic functional groups in different positions with respect to the quinoline group. IR spectra show that the azo compounds (HL_{*n*}) act as monobasic bidentate ligand by coordinating *via* the azodye (-N=N-) and oxygen atom of the phenolic group. The ESR (g_{\parallel} and g) and bonding α^2 parameters of the copper ion were greatly affected by substituting several groups position of ring of quinoline and *p*-aromatic ring. The ESR spectra of copper complexes in powder form show a broad signal with values in order $g_{\parallel} > g > g_e > 2.0023$. The value of covalency factor β and orbital reduction factor K accounts for the covalent nature of the complexes. All complexes possessed an octahedral and square planar geometry. The thermal properties of the complexes were investigated using TGA and DSC. It is found that the change of substituent affects the thermal properties of complexes.

Keywords: (4-alkylphenylazo)-5-sulfo-8-hydroxyquinolines (HL_{*n*}), Hydrogen-bonding stability, Supramolecular complexes, Spectroscopic studies, ESR, TGA and DSC.

*Abstracted from her M.Sc.

[†] Corresponding author Tel.: +20 1060081581; fax: +20 572403867.
E-mail address: elsonbatisch@yahoo.com (A.Z. El-Sonbati).

1. Introduction

Copper(II) complexes show a variety of stereochemistries and coordination numbers. Their flexibility is due to the d^9 configuration, where the nature of the $d_{x^2-y^2}$ orbital containing the unpaired electron imposes a strong Jahn-Teller effect [1].

The copper(II) ion exhibit great affinity for nitrogen donor ligands and quinoline complexes continue to be an intense field of investigation in coordination chemistry as bioinorganic models of metalloproteins and as catalysts of important industrial processes [2-5]. More recently the interest in the chemistry of azoquinoline ligand has been reborn due to their applications in supramolecular chemistry and new materials [4-10].

The coordination chemistry of quinoline and its azo derivatives have much attention by virtue of their applicability as potential ligands for large number of metal ions [7-10]. The metal chelates thus produced have wide applications in the dye industry, as analytical reagents for the microdetermination of metals and in biological uses [11]. Different methods were reported for the synthesis of azoquinoline [5-10]. The electronic and infrared (IR) spectra of a large number of azoquinoline were investigated for structure elucidation [8-10]. It was confirmed that these compounds exist mainly as a chelated hydrazo-keto structure but under the influence of high electron accepting substituents and in highly polar solvents, the azoquinoline compound was liable to exist in hydrazone-azo tautomeric equilibrium [5-7]. Nuclear magnetic resonance was used as a tool to determine the tautomeric forms of (4-methoxyphenylazo)-5-sulfo-8-hydroxyquinoline (HL_1), (4-methylphenylazo)-5-sulfo-8-hydroxyquinoline (HL_2), (4-phenylazo)-5-sulfo-8-hydroxyquinoline (HL_3), (4-chlorophenylazo)-5-sulfo-8-hydroxyquinoline (HL_4), (4-nitrophenylazo)-5-sulfo-8-hydroxyquinoline (HL_5) and several related azo heterocyclic in different solvents [10].

The design of new coordination supramolecules and polymers based on transition metals compounds and multidentate organic ligands has attracted much interest in recent years [12,13]. Depending on the nature of the metal and the coordination behaviour of the ligand one can develop synthetic strategies to influence the one-, two- or three-dimensional arrangement in the crystal in a more direct way [14]. Furthermore, it is now realized that weak hydrogen bond(s) that involve $O-H\cdots O$ and/or $N-H\cdots O$ hydrogen bond stacking interactions also play a significant and predictable structure determining role.

(4-alkylphenylazo)-5-sulfo-8-hydroxyquinoline (HL_n) and their related compounds (Fig. 1 A') have been extensively used as ligands in transition metal

coordination chemistry [15-19]. Ease of synthesis, favorable steric arrangement and variability of donor sites that these ligands possess with suitable constituents, make this family an excellent candidate for constructing new families of complexes which are of great intriguing interest for the coordination chemistry. Although, no structural chemistry or coordinating and biological studies have been reported on ligands containing both azo and quinoline function groups, data from our laboratory [15-19] have demonstrated that the bis-bidentate azodyes ligands play a key role in making new complexes with transition metal ions. However, little is known concerning the constituents of these complexes, as well as the chemistry involved in their preparation, or the structural and coordination in such complexes. It has been shown from the IR spectral data [14-22] that the hydrogen bonding plays an important role in biological systems. Due to the higher number of hydrogen bonds, the Watson-Crick pair of guanine and cytosine is more stable than the thymine-adenine complex [23]. Moreover, Jorgensen and El-Sonbati et al. [15-19,24] found out that the stability of multiple hydrogen bonded "dimers" depends not only on the number of hydrogen bonds but also on the hydrogen bonding pattern. The importance of clarifying the structure and stability of hydrogen-bonded complexes has opened up an area of surface science that has attracted a considerable attention in the environmental chemistry.

In this paper, we investigate the supramolecular chemistry of azo 8-hydroxy quinoline derivatives regarding the metal coordination as well as the behavior of hydrogen bonding of these molecules. These are achieved by reporting the studies of (i) the synthesis of novel (4-alkylphenylazo)-5-sulfo-8-hydroxyquinoline (HL_n) ligands, (ii) the synthesis of Cu(II)/Ni(II) complexes derived from this ligands, (iii) determining the vibrational mode of bonding, stability and structures of the hydrogen-bonding complexes, (iv) investigating the stereochemistry of the complexes based on the electronic spectra and other measurements, and (v) as well as study the thermal gravimetric analysis (TGA) and differential scanning calorimetry analysis (DSC) of Cu(II) complexes.

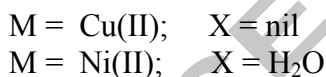
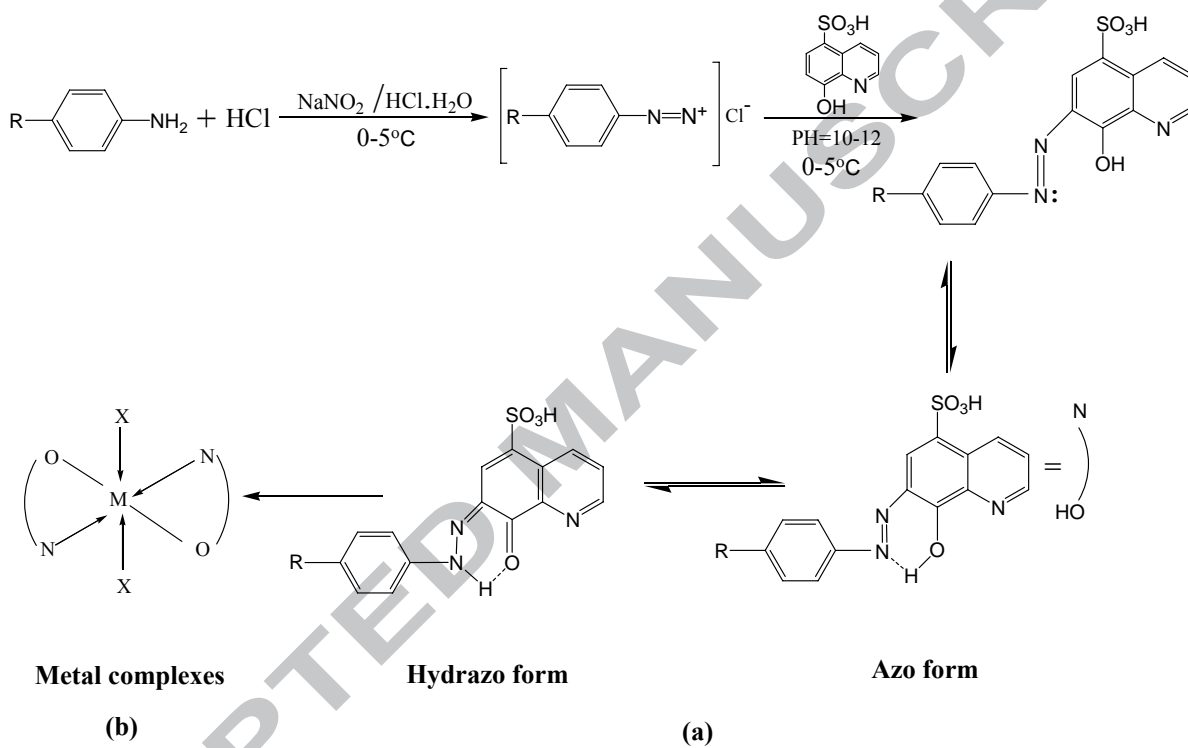
In addition to the above mentioned aims, we will discuss the previous studies of hydrogen bonding [16-18] and compare them with the results of the present paper in order to provide a better explanation and justification to the chemical behavior of such

complexes and biological allowing the reversible formation of aggregates which are non-covalently linked.

2. Experimental

2.1. Synthesis of ligands

The synthesis of ligand is summarized in Scheme 1. However detailed procedure is given in the following reactions:



n=1, R = OCH₃ (HL₁); n=2, CH₃ (HL₂); n=3, H (HL₃); n=4, Cl (HL₄); and n=5, NO₂ (HL₅)

Scheme 1. The formation mechanism of azodye ligands (HL_n).

The resulting formed ligands are:

(4-methoxyphenylazo)-5-sulfo-8-hydroxyquinoline (HL₁)

(4-methylphenylazo)-5-sulfo-8-hydroxyquinoline (HL₂)

(4-phenylazo)-5-sulfo-8-hydroxyquinoline (HL₃)

(4-chlorophenylazo)-5-sulfo-8-hydroxyquinoline (HL₄)

(4-nitrophenylazo)-5-sulfo-8-hydroxyquinoline (HL₅)

(4-alkylphenylazo)-5-sulfo-8-hydroxyquinolines (HL_n) were typically prepared by adding a 25 mL of distilled water containing hydrochloric acid (12 M, 2.68 mL, 32.19 mmol) were added to aniline (10.73 mmol) or *p*-derivatives. To the resulting mixture, stirred and cooled to 0 °C, a solution of sodium nitrite (10.73 mmol, in 20 mL of water) was added drop wise. The so-formed diazonium chloride was consecutively coupled with an alkaline solution (sulfonate) (10.73 mmol) in 20 mL of ethanol containing 602 mg (10.73 mmol) of potassium hydroxide. The red precipitate, which formed immediately was filtered and washed several times with water. The crude product obtained was purified by crystallization from hot ethanol (yield ~ 60-80%). The analytical data confirmed by expected composition, (Table 1). The ligands were also characterized by ¹H & ¹³C NMR and IR spectroscopy.

2.2. Synthesis of metal complexes

The appropriate ligand (0.01 mol) dissolved in ethanol (20 cm³) was added dropwise into an a ethanolic solution (20 cm³) of metal salt (0.01 mol) with stirring. After the complete addition, 0.50 g of sodium acetate was added to the solution and the reaction mixture was refluxed for 2 h. The solution, thus obtained was concentrated to half of its original volume by evaporation using a hot plate and allowed to cool to room temperature. During this, a microcrystalline solid was separated, which was isolated by filtration, washed with hot water followed by ethanol, ether and dried in air.

2.3. Analysis and physical measurements

All chemicals used were of highest available purity, were BDH, Analar, Sigma, or Merck products. Copper chloride dihydrates, nickel chloride hexahydrates, 5-sulfo-8-hydroxyquinoline, 4-alkylaniline, absolute ethyl alcohol, diethylether, dimethylformamide and dimethylsulfoxide. Concentrated nitric acid was reagent grade and used as supplied. Microanalyses of carbon, hydrogen, nitrogen and sulfur contents were performed in the Microanalytical Center, Cairo University, Egypt. Metal contents were determined complexometry after complete decomposition of their complexes with concentrated nitric acid in a Kjeldal flask, while the chlorine content was determined gravimetrically as AgCl [25]. Molar conductance measurements were measured in solutions of the metal complexes in DMF (10⁻³ M) using using Sargent Welch scientific Co., Skokie, IL, USA. X-ray diffraction patterns of [Cu(L₅)₂], is recorded on X-ray

diffractometer (Philips x'pert) with Ni-filtered CuK α -radiation ($\lambda = 1.5418 \text{ \AA}$) in the range of diffraction angle ($2\theta^\circ = 4-70^\circ$). The applied voltage and the tube current are 30 KV and 30 mA, respectively. The $^1\text{H-NMR}$ spectrum was obtained with a JEOL FX90 Fourier transform spectrometer with DMSO- d_6 as the solvent and TMS as an internal reference. Infrared spectra were recorded as KBr pellets using a Pye Unicam SP 2000 spectrophotometer. Ultraviolet-Visible (UV-Vis) spectra of the compounds were recorded in nuzol solution using a Unicam SP 8800 spectrophotometer. The magnetic moment of the prepared solid complexes was determined at room temperature using the Gouy's method. Mercury(II) (tetrathiocyanato)cobalt(II), $[\text{Hg}\{\text{Co}(\text{SCN})_4\}]$, was used for the calibration of the Gouy tubes. Diamagnetic corrections were calculated from the values given by Selwood [26] and Pascal's constants. Magnetic moments were calculated using the equation, $\mu_{\text{eff}} = 2.84 [\chi_M^{\text{corr.}}]^{1/2}$. ESR measurements of powdered samples were recorded at room temperature (Tanta University, Egypt) using an X-band spectrometer utilizing a 100 kHz magnetic field modulation with diphenyl picrylhydrazyle (DPPH) as a reference material. Thermal properties are investigated using Shimadzu Thermal Analyzer with a scan rate 10.0 $^\circ\text{C}/\text{minute}$ in air atmosphere in the temperature range 46-800 $^\circ\text{C}$.

3. Results and discussion

The physical properties of the ligands and the complexes are grouped in Tables 1 and 2. The elemental analysis data (Table 2) was found to agree well with the proposed formula of the complexes and confirmed the $[\text{Cu}(\text{L}_n)_2]$ composition with 1:2 [M:L] ratio. Generally all the complexes were colored, quite stable towards air, insoluble in water and common organic solvents but soluble in coordinated solvents. The Molar conductance values (Λ_m) of the complexes in DMSO ($1 \times 10^{-3} \text{ M}$) solution at 25 $^\circ\text{C}$ were found in the range 8.58-14.90 $\Omega^{-1} \text{ mol}^{-1} \text{ cm}^2$. These low values indicated that all of the complexes have non-electrolytic nature [27]. Hence, the molecular conductance measurements of the chelates confirm the proposed general formulae of those chelates as suggested depending upon the results of elemental analyses and IR spectra.

As shown in Tables 1 & 2, the values of yield % is related to the nature of the *p*-substituent as they increase according to the following order *p*-($\text{NO}_2 > \text{Cl} > \text{H} > \text{CH}_3 > \text{OCH}_3$). This can be attributed to the fact that the effective charge experienced by the d-electrons increased due to the electron withdrawing *p*-substituent (HL_4 and HL_5) while

it decreased by the electrons donating character of (HL₁ and HL₂). This is in accordance with that expected from Hammett's constants (σ^R) as in Fig. 2 correlate the yield % values with (σ^R), it is clear that all these values increase with increasing σ^R . The above results show clearly the effect of substitution in the *para* position of the benzene ring. It is important to note that the existence of a methyl and/or methoxy group enhances the electron density on the coordination sites and simultaneously decreases the values of yield %.

The X-ray diffraction spectrum of complex [Cu(L₅)₂] (**9**) is shown in Fig. 3. Spectrum of compound (**9**) exhibit many peaks with different intensities indicating polycrystalline nature.

3.1. Structure and stability

The presence of a sulfonate group in the quinoline ring confers special characteristics to the ligand, introducing changes in spectroscopic and structural properties of the metallic complexes.

It has been known [20-22,28,29] that 8-hydroxyquinoline exists, in solution, in a monomer dimer equilibrium. The results of this work suggest that in the monomeric form a strong intramolecular hydrogen bond is present. This is in agreement with a previous results [20-22,30]. The two such monomers lead to the dimer by forming an additional hydrogen bonding yielding the bifurcated hydrogen bonds and H-N-H nitrogen bridges (Fig. 1 A).

In addition to the two bifurcated intra/intermolecular OH---N hydrogen bonds (Scheme 1 and Fig. 4), two more intermolecular hydrogen bonding interactions are observed between nitrogen atom of azo/azomethine group and phenolic hydroxyl hydrogen oxygen atom. This additional H-bonding does not influence the intramolecular distance which shows a band at a lower frequency than the intermolecular interaction. Reason for this behavior might be due to the additional H-bond which influences the hydrogen bonding ability of the sulfonyl group by electronic and/or steric factors. The overall structure of the dimer is close to planar with a slight shift of the two quinoline units from the plane.

The two hydroxyquinoline units of the dimer (Fig. 1 B' & 1 C₂) are in one plane. The intermolecular as well as intramolecular hydrogen bonding occur between the hydroxyl group and the quinoline nitrogen atom. The intermolecular hydrogen bond

distance is shorter than the intramolecular one. This observation was also reported for other 8-hydroxyquinoline dimmers and might be due to an unflavored small O-H-N angle for the intramolecular interaction [29-31].

Hydrogen bonding represents one of the most versatile interactions that could be used for molecular recognition. In view of the large differences in the substituent effects (*e.g.*, the Hammett-type substituent constants for *p*-positions and sulfonyl group); it might be possible to tune the strength of the hydrogen bond effectively by linking the hydrogen-bonding site to a reaction center through a conjugated spacer, and by altering the charge state of the reaction center in the solution. At the hydrogen-bonding end, azo/azomethine is used as a proton acceptor to form a hydrogen bond with OH group of ligand.

An electron-withdrawing bridge would be expected to increase the acidity of the proton donor and hence increase its binding ability. As the electron-withdrawing character of an azo group is relevant to the interesting signal-amplifying behavior [32]. The results indicate that in the HL_n, the effects of the bridges are electron-withdrawing and electron-donating, respectively. Accordingly, the efficiency of sp²-hybridized bridges is N=N > C=N.

Coggeshall [33] and El-Sonbati et al. [16-22] found three kinds of bonded –OH structures on the basis of the frequencies: i) only the oxygen is in the bridge while the hydrogen is free, ii) a polymer chain is formed in which both hydrogen and oxygen atoms participate in the hydrogen bond, iii) dimer associates are formed. Intramolecular hydrogen bond between the nitrogen atom of C=N(CN_{py})/–N=N– (five/six-membered) system and hydrogen atom of the phenolic hydroxyl hydrogen atom and hydrogen (C₈-OH) are illustrated in (Fig. 1 B, C and C'). Intermolecular hydrogen bonding can form cyclic dimer through the O-H---OH type between C₈-OH/N=N of one molecule and C₈-OH/N=N group of another one (Fig. 4 H, G & F) and/or ---N type between C₈-OH of one molecule and CN_{py}/–N=N– of another (Fig. 4 D).

In general, hydrogen bonding involving OH groups are proton donors and their O atoms are proton acceptors. Both intra and intermolecular OH-N may form a number of structures in a simultaneous equilibrium.

3.2. ^1H & ^{13}C NMR spectra

The ^1H NMR spectra of all the ligands were recorded in DMSO- d_6 at room temperature. The signal due to methyl and methoxy proton appeared as singlet at 1.55 and 3.84 ppm, respectively. In the aromatic region, a few doublets and in few cases some overlapping doublets/multiplets are observed in the range δ 6.78-8.40 ppm ($J = 12$ Hz). These doublets/multiplets are due to aryl protons of three benzene rings. Another singlet corresponding to one proton for all compounds is observed in the range $\delta \sim 9.2$ -10.40 ppm. This signal disappeared when a D_2O exchange experiment was carried out. It can be assigned either to OH or NH, in either case; it is strongly deshielded because of formation of strong hydrogen bonding with the other atom (N/O) (Figs. 1 & 4). It may be noted that the integration of this signal perfectly matches with one proton and there is no other fragment(s) of this signal, which suggests that only one tautomeric form of the ligand exist in solution under the experimental conditions. Comparing with the solid state study, we prefer to assign this signal to OH, however, assignment of this peak to NH cannot be ruled out provided solid state structural evidence is not considered [34]. As reported in a previous study [36], this hydrogen bonding leads to a large deshielding of these protons. The shifts are in the sequence: $p\text{-NO}_2 > p\text{-Cl} > \text{H} > p\text{-OCH}_3 > p\text{-CH}_3$. The appearance of signals due to $\text{HC}=\text{N}$ [~ 8.94 ppm (1H)] protons of the same positions in the ligand.

The assignments made from ^1H & ^{13}C NMR spectrum of the ligand (HL_5) are shown in Table 3.

3.3. Characterization of the complexes

Infrared spectra

The significant IR bands with the tentative assignments of the HL_n and copper(II) complexes are presented in Table 4. The characteristic IR bands of the complexes differ from their uncomplexed HL_n and provide significant indications regarding the coordination and bonding sites of the ligand. The IR spectroscopy is known to be a powerful tool for structural determinations of the ligand and metal chelates.

By tracing the IR spectra of the azo compounds, no NH_2 stretching vibrations are apparent. This supports the formation of azodye ligands. The mode of bonding of the HL_n to the metal ions was elucidated by investigating the IR spectra of the complexes on the basis of a comparative analysis of the results with respect to literature data of related

systems. The positions of the most relevant and characteristic bands are due to: i) azo nitrogen, ii) OH group and iii) CN_{py} group.

Much has been discussed about the –OH stretching frequency and intensity of phenol derivatives depending on many factors (*e.g.*, constituents, medium, *etc.*). Hoyer [37] reviewed the relationship between the hydrogen bond band and the –OH stretching frequency. In addition to that, there have been many other research workers who examined the problem in finer and more quantitative data. This has attracted our attention to acquire the IR technique to explain and justify the bonding in this study.

The IR spectrum of the ligands showed bands at 3390-3410 and 1285-1295 cm⁻¹ that may be assigned to $\nu(\text{OH})$ and $\nu(\text{C-O})$ phenolic, respectively. This latter band was shifted to higher frequencies (1345-1358 cm⁻¹) in the complexes, confirms that the C₈-OH group takes part in the complex formation through O⁻ owing to strong hydrogen bonding both intramolecular [O-H...N (Fig. 1 B), O-H...N (Fig. 1 C)] and intermolecular hydrogen bonding of the O-H...N type between N=N of one molecule and OH group of another one (Fig. 4 E), the frequency of the hydrogen bonded OH is probably lowered to considerable extent and overlaps with the OH vibrations, thus appearing as a broad band in the region 3390-3410 cm⁻¹ [10,28]. All the complexes exhibit $\nu(\text{C=C})$ in 1498 cm⁻¹. The presence of a *p*-substituted benzene ring in the ligands as well as in the complexes is indicated by strong and sharp bands around 720-740 cm⁻¹. Bands at 2950-3040 cm⁻¹ for the ligands and at ~ 2960-3040 cm⁻¹ for the complexes are assigned to $\nu(\text{C-H})$ vibrations of the aromatic system. This is also in agreement with the data reported by El-Sonbati and co-workers [16-22,36].

The assignment of the 1570 cm⁻¹ (N=N) and 1585 cm⁻¹ (CN) (non-bonded groups) stretching modes is based on our previous work [16-22], El-Sonbati et al. [35] and Henry et al. [38]. Comparing the position of these bands for the different ligands, it is obvious that ring substitution results in a shift to lower frequencies. This behavior can probably be explained by the lowering in the electronic density caused by electronegative groups.

1570 cm⁻¹ (N=N) occurs at higher frequency in the ligands than in the respective complexes by 20-35 cm⁻¹, revealing its involvement in complexation [20-22]. In this case, the decrease of the electronic density of the ring may be correlated with the donor character of the oxygen and/or N atoms in the M-O and M-N bond. These is also another correlation, observed when comparing the position of the $\nu(\text{N=N})$ band in the free ligand

and in the corresponding complexes. In these cases, the higher shift corresponds to higher electronegativity. Evidently, the presence of electronegative groups in the ring affects the donor capacity of the O and N atoms. The coordination of the azo-nitrogen and phenolic oxygen were further supported by the appearance of two non-ligand bands. According to Stefov et al. and El-Sonbati et al. [35,39], coordinated water should exhibit frequencies at ~ 830 , ~ 570 and ~ 495 cm^{-1} . The absence of spectral bands in these regions in the spectra of complexes **1**, **3**, **5**, **7** and **9** indicates that the water molecules in these complexes are not coordinated. These were not present in the spectra of the ligands. From the above arguments together with the elemental analysis, it was concluded that ligands behave as a monobasic bidentate azo dye ligands with NO donor sites.

These comparisons show that the electronegativity of the ring substituents produces not only a decrease of the electronic density over the ring, generating a diminution in the (N=N) stretching frequency, but also causes a lowering of the donor character of the N atom.

3.4. Electronic spectra

In general, most of the azo compounds give spectral localized bands in the wavelength range 46620-34480 and 31250-270370 cm^{-1} . The first region is due to the absorption of the aromatic ring compared to 1B_b and 1L_b of mono substituted benzene and the second region is due to the conjugation between the azo group and the aromatic nuclei with intermolecular charge transfer resulting from π -electron migration to the diazo group from electron donating substituents. The *p*-substituents increase the conjugation with a shift to a longer wavelength. Most of the simple *p*-substituted compounds are in the azoid form in cyclohexane and alcohols. The substituted effect is related to the Hammett's constants values [13,21]. The position of the $\pi \rightarrow \pi^*$ transition of the azo groups remains as one of the more interesting unanswerable questions of molecular spectroscopy. For azo benzenes, as the possibilities of the mesomerism became greater, the stabilization of the excited state is increased relative to that of the ground state and a bathochromic shift of the absorption bands follow [13]. Based on MO theory [40] the energy terms of the molecular orbital became more closely spaced as the size of the conjugated system increases. Therefore, with every additional conjugated double bond the energy difference between the highest occupied and the lowest vacant

electron level became smaller and the wavelength of the first absorption band corresponds to this transition is increased. The azo group can act as a proton acceptor in hydrogen bonds [13,21]. The role of hydrogen bonding in azo aggregation has been accepted for some time.

HL_n exhibited bands at 32500-32150 cm⁻¹ (CN) (- *), 33450-33340 cm⁻¹ (H-bonding and association), 40038-39460 cm⁻¹ (phenyl) (Ph-Ph*, - *) [13,41] and 29340-29230 cm⁻¹ transition of phenyl rings overlapped by composite broad (- *) of azo structure. The band due to the n → * transition obtained in the visible region is associated mainly with the color of the respective compound [13]. The band due to * transition moves to lower energy. The last band in the visible range is considered as being due to an intramolecular charge transfer involving the rote molecule in analogy to the behavior of azomethine compound [36]. These shifts or the disappearance of the bands are indicative of coordination of the ligands to M(II). The position of their bands is varied from one dye to the other which may be due attributed to the *p*-phenylazo substituent variable donating power.

The nickel(II) complexes displayed three bands 8860-8890 cm⁻¹ [³A_{2g} → ³T_{2g} (F)]ν₁, 14840-14960 cm⁻¹ [³A_{2g} → ³T_{1g} (F)]ν₂ and 25000-25105 cm⁻¹ [³A_{2g} → ³T_{1g} (P)]ν₃, transitions, suggestive of octahedral geometry [42]. The value of transition ratio ν₂/ν₁ and β lies in ~ 1.677 and ~ 0.85 cm⁻¹ providing further evidence for octahedral geometry for nickel(II) complexes. The β values for the complexes are lower than the free ion value, thereby indicating orbital overlap and delocalization of d-orbitals. The β-values obtained are less than unity suggestive considerable amount of covalent character of the metal-ligand bonds. Nickel(II) complexes are paramagnetic and the room temperature magnetic moment value 2.94-3.15 B.M. corresponding to three unpaired electron and in the range of octahedral nickel(II) complexes [43].

For square planar complexes, the lower energy d-d bands is usually observed in the region 18280-16000 cm⁻¹ nm. The complexes reported in the present work show the lower energy d-d band in the region 15575-13640 cm⁻¹, and this red shift may be due to the tetrahedral distortion from square planar environment of the Cu(II) ion [44]. This behavior probably due to the steric effects of the bulky group in the pyridine of the ligands. Copper(II) complexes are paramagnetic and the room temperature magnetic moment values ranging from 1.76 to 1.86 B.M. are close to the spin only value of 1.70

B.M. indicate the presence of one unpaired electron and demonstrate that these complexes are monomeric in nature and the presence of metal-metal interaction.

3.5. ESR spectra

ESR spectra of the polycrystalline powders were recorded at room temperature. The values of g factors were assessed following the method described by Searl et al. [45] and are presented in Table 5. The g tensor values of Cu(II) complex can be used to derive the ground state. In tetragonal and square planar complexes the unpaired electron lies in the $d_{x^2-y^2}$ orbital giving ${}^2B_{1g}$ as the ground state with the $g_{||} > g > 2.0023$ [44]. From the observed values for complexes (1, 5 & 9), it is clear that $g_{||} > g$. These data are in agreement with those obtained from the electronic spectra and confirm the square planar geometry. The term of the fundamental state is thus defined by the obtained $d_{x^2-y^2}$. The g -values are related by the expression [44], $G = g_{||} - 2/g - 2$. If $G > 4.0$, then local tetragonal axes are aligned parallel or only slightly misaligned, the exchange interaction are neglected, if $G < 4.0$, suggesting $d_{x^2-y^2}$ ground state with a small exchange coupling [44], i.e. it is considered the existence of some exchange interaction between the Cu(II) centers. Thus, in case of complexes (5) and (9), the geometric parameter $G = 3.73$ and 3.29 , respectively, confirmed the existence of some exchange interactions between the Cu(II) centers. The observed value for the exchange interaction parameter for the complex (1) was greater than 4.0 ($G = 4.24$) which confirmed the subsistence of no exchange interaction between the Cu(II) centers. These results were further supported by their magnetic moments. The empirical ratio $g_{||}/A_{||}$ was frequently used to evaluate distortions in tetra coordinated copper(II) complexes [44]. The close to 100, indicated a roughly square planar structure around the copper(II) ion [44] and the values from 170 to 250 indicated a distorted tetrahedral geometry. Hence, the value of the $g_{||}/A_{||}$ ratio for Also, the $g_{||}/A_{||}$ value considered as a diagnostic of stereochemistry [44], the range reported for square planar complexes, are 105 to 135 cm^{-1} and for tetragonal distorted complexes 150 to 250 cm^{-1} . The $g_{||}/A_{||}$ values lie just within the range expected for the complexes.

The g -values of the copper(II) complexes with a ${}^2B_{1g}$ ground state ($g_{||} > g$) may be expressed [21,44] by

$$g_{||} = 2.0023 - (8K_{||}^2\lambda^0/\Delta E_{xy})$$

$$g = 2.0023 - (2K\lambda^0/\Delta E_{xz})$$

where $K_{||}$ and K are the parallel and perpendicular components respectively of the orbital reduction factor (K), λ^0 is the spin-orbit coupling constant for the free copper, ΔE_{xy} and ΔE_{xz} are the electron transition energies of ${}^2B_{1g} \rightarrow {}^2B_{2g}$ and ${}^2B_{1g} \rightarrow {}^2E_g$. From the above relations, the orbital reduction factors ($K_{||}$, K , K), which are a measure of covalency [21,44], can be calculated. For an ionic environment, $K = 1$ and for a covalent environment $K < 1$, the lower value of K , the greater is the covalent.

$$K^2 = (g - 2.0023) \Delta E_{xz}/2\lambda^0$$

$$K_{||} = (g_{||} - 2.0023) \Delta E_{xy}/8\lambda^0$$

$$K^2 = (K_{||}^2 + 2K^2)/3$$

The observed $K_{||}$ (0.68 – 0.77) $<$ K (0.69-0.95) relation indicated the presence of significant in-plane π -bonding. Thus, the ESR study of the copper(II) complex has provided supportive evidence to the conclusion obtained on the basis of electronic spectrum and magnetic moment value.

K for the copper(II) complexes are indicating of their covalent nature [46,47]. Kivelson and Neiman [48] noted environment, $g_{||} < 2.3$. Theoretical work by Smith [49] seems to confirm this view. The $g_{||}$ -values reported here show considerable covalent bonding character [21,44]. Also, the in-plane σ -covalency parameter $\alpha^2(\text{Cu})$ was calculated by

$$\alpha^2 = A_{||}/P + (g_{||} - 2.0023) + 3/7 (g - 2.0023) + 0.04$$

The in-plane and out-of-plane π -bonding coefficients (β_1^2 & β^2), respectively are dependent upon the values of ΔE_{xy} and ΔE_{xz} in the following equations [21]

$$\alpha^2\beta^2 = (g - 2.0023) \Delta E_{xz}/2\lambda^0$$

$$\alpha^2\beta_1^2 = (g_{||} - 2.0023) \Delta E_{xy}/8\lambda^0$$

In this work, the complexes show β_1^2 values 1.03, 0.97 and 0.93 indicating a moderate degree of covalence in the in-plane π -bonding, while β^2 are 1.05, 1.33 and 1.22 indicating ionic and covalent character of the out-of-plane π -bonding [21].

The ESR study of the Cu(II) complexes has provided supportive evidence to the conclusion obtained on the basis of electronic spectrum and magnetic moment value. The plot of $(\beta_2)^2$ and $(\beta_1)^2$ vs. of (σ^R) gives straight line with increase the value of (σ^R)

decrease $(\beta_2)^2$ and increase the $(\beta_1)^2$ (Fig. 5). It seems that the electron withdrawing *p*-substituent increase the positive charge on the metal ion leading to a increase in $g_{||}$ and $A_{||} \times 10^{-4} \text{ cm}^{-1}$ and subsequently a increase in (σ^R) (Fig. 6). In addition, Fig. 7 shows clearly that the shift is in the direction to that of 2 and g_{iso} .

The above results show clearly the effect of electron density on the ESR parameter on the stereochemistry of Cu(II) complexes. It is important to note that the existence of high electron density enhances and activate the coordination sites and simultaneously increases the value of ESR parameters (Table 5).

3.6. Thermal studies

The thermal properties of the copper(II) complexes of ligands (HL_n) were investigated by thermogravimetric analysis (TGA) and differential scanning calorimetry (DSC) in the temperature range 46-800 °C are shown in Fig. 8. The thermal analyses data for the copper(II) complexes are summarized in Table 6. It can be seen that the TG curves of the complexes show mass loss down to 150 °C, indicating the presence of adsorptive solvent molecules in the coordination sphere. The TG curves of the complexes show that for the copper(II) complexes three steps of the losses of mass. The DSC data for copper(II) complexes show many exothermic peaks except $[Cu(L_5)_2]$ complex show one exothermic peak as shown in Fig. 8. These peaks can be explained in terms of TGA curves [50]. According to literature the azo bonds in the azo metal complexes breakdown when the temperature is higher than 250 °C resulting in the exothermic peaks [51].

For the $[Cu(L_1)_2]$ complex the recorded DSC curve show three exothermic peaks at ~ 338.8, 393.7 and 439.2 °C. Simultaneously, the recorded DSC curve of the $[Cu(L_2)_2]$ complex show three exothermic peaks at 270.3, 364.1 and 520.5 °C, while the recorded DSC curve of the $[Cu(L_3)_2]$ complex show only two exothermic peaks at 281.8 and 453.4 °C. For the $[Cu(L_4)_2]$ complex the recorded DSC curve show three exothermic peaks at 279.6, 378.3 and 506.5 °C and for the $[Cu(L_5)_2]$ complex the recorded DSC curve show only one peak at 360.1 °C (Fig. 8).

The effective activation energies of the thermal degradation of copper(II) complexes were determined using TGA thermograms. The rate constant of the thermal degradation plotted according to the Arrhenius relationship equation: [52]

$$\ln K = \ln A - E_a/RT,$$

where K is the rate constant of the thermal degradation in the initial stages of decomposition, A is a constant, R is the gas constant ($= 8.314 \text{ JK}^{-1} \text{ mol}^{-1}$), T is the absolute temperature and E_a is the thermal activation energies of degradation. The values of the thermal activation energies of degradation for copper(II) complexes are calculated from the slope of the straight line obtained from the plot $\ln K$ versus $1/T$ as shown in Fig. 9. The values E_a for $[\text{Cu}(\text{L}_1)_2]$, $[\text{Cu}(\text{L}_2)_2]$, $[\text{Cu}(\text{L}_3)_2]$, $[\text{Cu}(\text{L}_4)_2]$ and $[\text{Cu}(\text{L}_5)_2]$ are found to be 62.27, 141.55, 139.23, 74.79, and 44.70 kJ/mol, respectively. The $[\text{Cu}(\text{L}_3)_2]$ and $[\text{Cu}(\text{L}_2)_2]$ have the highest value of E_a . This indicates that, $[\text{Cu}(\text{L}_3)_2]$ and $[\text{Cu}(\text{L}_2)_2]$ are more thermally stable than the other complexes [53].

4. Conclusion

The results arising from the present investigations confirm that the hydroxyquinoline exist, in solution, in a monomer dimer equilibrium. The results suggest that in the monomeric form a strong intramolecular hydrogen bond is present. Two monomers lead to the dimer by formation of additional hydrogen bonding yielding the bifurcated hydrogen bonds and H-N-H nitrogen bridges (Fig. 1 A). The dimer is able to dissociate, while the intramolecular interaction can be broken if appropriate hydrogen bond acceptors are attached which acts as competitors to the quinoline nitrogen atoms as was observed (Fig. 1 B'). In conclusion, the results of the present study indicate that the selected (4-alkylphenylazo)-5-sulfo-8-hydroxyquinoline (HL_n) ligands are suitable for building a supramolecular structure. Moreover, since the azo and/or hydrazo compounds experience photochemical isomerization and are, therefore, of interest for applicative purposes.

The satisfactory analytical data coupled with the studies presented above indicate that the complexes under this investigation are of the general composition, $[\text{M}(\text{L}_n)_2\text{X}]$ [$\text{M} = \text{Cu}$; $\text{X} = \text{nil}$ or $\text{M} = \text{Ni}$; $\text{X} = \text{H}_2\text{O}$], where $\text{HL}_n = (4\text{-alkylphenylazo})\text{-5sulfo-8-hydroxyquinoline}$. In view of the well characterized of bis[(4-alkylphenylazo)-5-sulfo-8-hydroxyquinoline] $\text{Cu}(\text{II})/\text{Ni}(\text{II})$ (involving a monoprotic bidentate (O, N-donor) azo ligand, square planar/octahedral structures with O, N-donor at the equatorial positions in *cis*-arrangement have been proposed for these complexes. It is also clear that these ligands have high affinity for chelation with metal ions under study due to the increasing charge density of the metal ion and hence to the increasing of their coordination affinities.

The present study demonstrates perfectly an application of IR spectra and molecular modeling in revealing not only the multiple inter/intramolecular of π - π stacking among the aromatic groups as well as the hydrophobic interactions among hydrogen bonding species between hydrazide moieties involving in a series of novel hydrazide based azo quinoline derivatives.

Further studies with the title ligand, using different metal ions, are in progress and will be published in course.

ACCEPTED MANUSCRIPT

Table 1Elemental analysis (C, H, S and N)^a, color and yield (%) of the ligands.

Compound ^b	M ⁺	Color	Yield (%)	Exp. (Calcld.)%			
				C	H	N	S
HL₁ (C ₁₆ H ₁₃ N ₃ O ₅ S)	358	Black	60.4	53.88 (53.48)	3.82 (3.62)	12.21 (11.70)	9.35 (8.91)
HL₂ (C ₁₆ H ₁₃ N ₃ O ₄ S)	343	Red	62.0	56.12 (55.98)	3.90 (3.79)	12.72 (12.25)	9.71 (9.33)
HL₃ (C ₁₅ H ₁₂ N ₃ O ₄ S)	329	Pale red	64.7	54.87 (54.71)	3.45 (3.34)	13.22 (12.77)	10.10 (9.73)
HL₄ (C ₁₅ H ₁₀ N ₃ O ₄ SCI)	363.5	Red	68.8	49.64 (49.52)	2.84 (2.75)	11.93 (11.55)	9.21 (8.80)
HL₅ (C ₁₅ H ₁₀ N ₄ O ₆ S)	374	Dark red	78.0	48.30 (48.13)	2.72 (2.67)	15.30 (14.97)	8.83 (8.56)

^aThe excellent agreement between calculated and experimental data supports the assignment suggested in the present work, insoluble in water and partially in common organic solvents but soluble in coordinated solvents.

^bHL₁– HL₅ are the ligands as given in Scheme 1.

Table 2Elemental analysis^a, yield (%) and magnetic moment data of complexes

Compound ^b	Yield (%)	μ_{eff} (B.M.)	Exp.(Calcld.)%			
			C	H	N	M
[Cu(L ₁) ₂] (1)	60.2	1.76	49.19 (49.26)	2.95 (3.08)	10.57 (10.78)	7.89 (8.15)
[Ni(L ₁) ₂ (OH ₂) ₂] (2)	41.2	2.94	47.42 (47.37)	3.50 (3.45)	10.61 (10.36)	7.45 (7.24)
[Cu(L ₂) ₂] (3)	70.2	1.78	51.19 (51.47)	3.07 (3.21)	10.89 (11.24)	8.34 (8.50)
[Ni(L ₂) ₂ (OH ₂) ₂] (4)	47.6	2.96	49.45 (49.31)	3.68 (3.60)	11.10 (10.79)	7.76 (7.54)
[Cu(L ₃) ₂] (5)	72.2	1.82	50.12 (50.03)	2.66 (2.78)	11.42 (11.67)	8.62 (8.83)
[Ni(L ₃) ₂ (OH ₂) ₂] (6)	54.0	2.98	48.20 (47.96)	3.27 (3.20)	11.46 (11.19)	8.36 (7.82)
[Cu(L ₄) ₂] (7)	76.5	1.85	45.55 (45.65)	2.17 (2.28)	10.41 (10.65)	5.88 (8.06)
[Ni(L ₄) ₂ (OH ₂) ₂] (8)	56.9	3.13	44.06 (43.92)	2.73 (2.58)	10.56 (10.25)	7.50 (7.15)
[Cu(L ₅) ₂] (9)	79.0	1.86	44.29 (44.47)	2.10 (2.22)	13.60 (13.84)	7.62 (7.85)
[Ni(L ₅) ₂ (OH ₂) ₂] (10)	67.4	3.15	42.75 (42.72)	2.94 (2.85)	13.58 (13.29)	7.33 (6.97)

^aThe excellent agreement between calculated and experimental data supports the assignment suggested in the present work.

^bL₁ – L₅ are the anions of the ligands HL₁ – HL₅ as given in Scheme 1.

Table 3¹³C NMR and ¹H NMR spectrum for HL₅ (ppm vs. TMS)^a.

HL ₅ ^b	¹³ C NMR δ, ppm (C atoms, peak assignment)	¹ H NMR δ, ppm (H atoms, peak assignment)
14	157.7	-
11	157.7	-
08	147.2	9.87
02	147.0	8.44
05	146.5	-
07	136.9	-
04	135.9	8.77
13	124.9	8.26
15	124.9	8.26
06	123.6	8.26
12	121.1	7.77
16	121.1	7.77
03	116.9	7.38
09	128.2	-
10	129.4	-

^a The excellent agreement experimental data supports the assignment suggested in the present work.

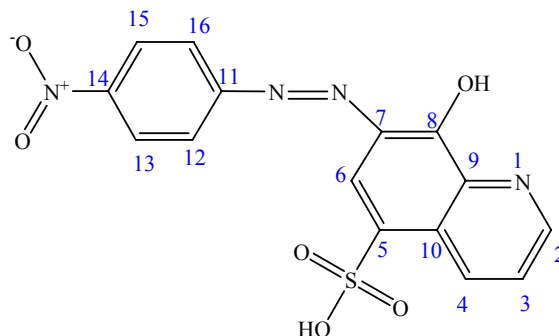


Table 4The infrared (cm^{-1}) data of the azodye ligands (HL_n) and their complexes

Compound ^a	$\nu(\text{OH})$	$\nu(\text{C-O})$	$\nu(\text{M-O})$	$\nu(\text{M-N})$	$\nu(\text{OH}_2)$
HL₁	3390	1265	-	-	-
1	-	1345	420	510	-
2	-	1343	465	508	830,570,495
HL₂	3395	1287	-	-	-
3	-	1347	425	518	-
4	-	1349	470	517	833,572,495
HL₃	3340	1290	-	-	-
5	-	1350	428	524	-
6	-	1352	476	522	836,575,498
HL₄	3405	1293	-	-	-
7	-	1353	433	527	-
8	-	1354	479	526	842,580,505
HL₅	3410	1295	-	-	-
9	-	1355	438	532	-
10	-	1357	484	530	850,585,508

^a Numbers as given in Table 2.

Table 5

ESR parameters for the copper(II) complexes

Complex ^a	g_{\parallel}	g_{\perp}	g_{iso}	A_{\parallel}^b	A_{iso}^b	G	$g_{\parallel}/A_{\parallel}$	ΔE_{xy}	ΔE_{xz}	K_{\parallel}	K_{\perp}	K	α^2	β^2_{\perp}	β^2
1	2.247	2.06	2.122	126	213	4.24	178	18320	19800	0.68	0.69	0.69	0.66	1.03	1.05
5	2.255	2.07	2.132	147	226	3.73	153	18522	20085	0.71	0.82	0.78	0.73	0.97	1.13
9	2.258	2.08	2.139	159	242	3.29	142	18585	20212	0.72	0.95	0.87	0.77	0.93	1.22

^aNumbers as given in Table 2.^bExpressed in units of cm^{-1} multiplied by a factor of 10^{-4}

Table 6

The thermal analyses data for the copper(II) complexes.

Complex ^a	First stage		Second stage		Third stage		Remaining Wt loss% after 650 °C
	Temp.	Wt	Temp.	Wt	Temp.	Wt	
	°C	loss%	°C	loss%	°C	loss%	
1	190	10.4	300	29.8	345	45.2	9.9
3	250	8.2	331	7.8	378	50.1	26.0
5	260	4.7	285	19.3	419	55.9	13.2
7	254	6.3	286	11.5	393	49.5	23.1
9	215	6.5	270	30.9	325	49.9	9.5

^aNumbers as given in Table 2.

Remaining Wt loss% corresponding to metal oxides.

References

- [1] R.J. Deeth, M.A. Hitchman, *Inorg. Chem.* 25 (1986) 1225-1233.
- [2] N. Gupta, R. Gupta, S. Chandra, S.S. Bawa, *Spectrochim. Acta A* 61 (2005) 1175-1180.
- [3] N.K. Singh, A. Srivastava, A. Sodhi, P. Ranjan, *Transition Met. Chem.* 25 (2000) 133-140.
- [4] M.S. Azziz, A.Z. El-Sonbati, A.S. Hilali, *Chem. Pap.* 56 (2002) 305-308.
- [5] A.Z. El-Sonbati, A.S. Al-Shihri, A.A. El-Bindary, *Inorg. & Organom. Polym.* 14 (2004) 53-71.
- [6] A.A. El-Bindary, A.Z. El-Sonbati, *Polish J. Chem.* 74 (2000) 615-620.
- [7] A.A. Al-Sarawy, A.A. El-Bindary, A.Z. El-Sonbati, M.M. Makpel, *Polish J. Chem.* 80 (2006) 289-295.
- [8] A.Z. El-Sonbati, A.A. Al-Sarawy, M. Moqbel, *Spectrochim. Acta A* 74 (2009) 463-468.
- [9] A.Z. El-Sonbati, A.A. El-Bindary, E.M. Mabrouk, R.M. Ahmed, *Spectrochim. Acta A* 57 (2001) 1751-1757.
- [10] A.Z. El-Sonbati, A.A. El-Bindary, R.M. Issa, H.M. Kera, *Desig. Mon. and Polym.* 7 (2004) 445-459.
- [11] A.Z. El-Sonbati, R.M. Issa, A.M. Abd El-Gawad, *Spectrochim. Acta Part A* 68 (2007) 134-138.
- [12] A.Z. El-Sonbati, M.A. Diab, A.A. El-Bindary, M.K. Abd El-Kader, *Spectrochim. Acta A* 99 (2012) 211-217.
- [13] A.Z. El-Sonbati, M.A. Diab, M.S. El-Shehawy, M. Moqbal, *Spectrochim. Acta A* 75 (2010) 394-405.
- [14] A.A. El-Bindary, A.Z. El-Sonbati, E.H. El-Mosalamy, R.M. Ahmed, *Chem. Pap.* 57 (2003) 255-258.
- [15] N.H. Patel, H.M. Parekh, M.N. Patel, *Transition Met. Chem.* 30 (2005) 13-17.
- [16] A.Z. El-Sonbati, A.A. Belal, S.I. El-Wakel, M. A. Hussien, *Spectrochim. Acta A* 60 (2004) 965-972.
- [17] A.Z. El-Sonbati, R.M. Issa, A.M. Abd El-Gawad, *Spectrochim. Acta A* 74 (2009) 463-468.

- [18] A.Z. El-Sonbati, A.S. Shihri, A.A. Bindary, *Spectrochim. Acta A* 60 (2004) 1763-1768.
- [19] A.Z. El-Sonbati, A.A. El-Bindary, A.F. Shoair, *Spectrochim. Acta A* 58 (2002) 3003-3009.
- [20] A.Z. El-Sonbati, A.A. El-Bindary, A.A. Sarawy, *Spectrochim. Acta A* 58 (2002) 2771-2778.
- [21] A.Z. El-Sonbati, M.A. Diab, M.M. El-Halawany, N.E. Salam, *Mater. Chem. & Phys.* 123 (2010) 439-449.
- [22] A.Z. El-Sonbati, M.A. Diab, M.M. El-Halawany, N.E. Salam, *Spectrochim. Acta A* 77 (2010) 795-801.
- [23] P. Jurečka, P. Hobza, *J. Am. Chem. Soc.* 125 (2003) 15608-15613.
- [24] W.I. Jorgensen, J. Pranata, *J. Am. Chem. Soc.* 112 (1990) 2008-2010.
- [25] J. Bassett, R.C. Denney, G.H. Jeffery, J. Mendham, *Vogel's Textbook of Quantitative Inorganic Analysis*, fourth ed., Longmans, London, 1978.
- [26] P.W. Selwood, *Magnetic Chemistry*, Interscience Pub. Inc., New York, 1956.
- [27] J.A. Deen, *Lange's Hand Book of chemistry*, fourthed, Springer, Bertin, 1992.
- [28] M.A. Diab, A.A. El-Bindary, A.Z. El-Sonbait, O.L. Salem, *Mol. Struct.* 1007 (2012) 11-19.
- [29] M. Albrecht, O. Blau, E. Wegelins, K. Rissanen, *New J. Chem.* 23 (1999) 667-673.
- [30] G. Cook, V.M. Rotello, *Chem. Soc. Rev.* 31 (2002) 275-286.
- [31] M. Albrecht, K. Witt, E. Wegelins, K. Rissanen, *Tetrahedron* 56 (2000) 591-594.
- [32] H. Suzuki, "Electronic Absorption Spectra and Geometry of Organic Molecules", Academic Press, New York, 1967.
- [33] N.D. Coggeshell, *J. Am. Chem. Soc.* 69 (1947) 1620-1624.
- [34] R.N. Jadeja, J.R. Shah, E. Suresh, P. Paul, *Polyhedron* 23 (2004) 2465-2474.
- [35] A.Z. El-Sonbati, A.A. Belal, M.A. Diab, M.Z. Balboula, *Spectrochim. Acta A* 78 (2011) 1119-1125.
- [36] A.Z. El-Sonbati, *Spectrosc. Lett.* 30 (1997) 459-472.
- [37] H. Hoyer, *Z. Electrochem.* 36 (1980) 97-101.
- [38] R.P. Henry, P.C.H. Mitchell, J.E. Pure, *Inorg. Chim. Acta* 7 (1975) 885-892.
- [39] V. Stefov, B. Šoptrajanov, V. Petruševski, *Mol. Struct.* 293 (1993) 97-100.
- [40] Y. Jean, "Molecular Orbitals of Transition Metal Complexes" Oxford, Université Paris-Sud, 2004.

- [41] A.Z. El-Sonbati, A.A.M. Belal, M.S. El-Gharib, Sh.M. Morgan, *Spectrochim. Acta* 95 (2012) 627-636.
- [42] A.B.P. Lever, "Inorganic Electronic Spectroscopy", Elsevier, New York, 1968.
- [43] B.N. Figgis, J. Lewis, "Modern Coordination Chemistry", Interscience, New York, 1967.
- [44] A.Z. El-Sonbati, A.A. El-Bindary, M.A. Diab, S.G. Nozha, *Spectrochim. Acta A* 83 (2011) 490-498.
- [45] J.W. Searl, R.C. Smith, S.J. Wyard, *Proc. Phys. Soc.* 78 (1961) 1174-1176.
- [46] J.M. Assour, *J. Chem. Phys.* 43 (1965) 2477-2489.
- [47] S.E. Harrison, *J. Chem. Phys.* 40 (1964) 365-370.
- [48] D. Kivelson, R. Neiman *J. Chem. Phys.* 35 (1961) 149-155.
- [49] D.W.J. Smith, *Chem. Soc. (A)* (1970) 3108-3116.
- [50] X. Li, Y. Wu, D. Gu, F. Gan, *Dyes and Pigments* 86 (2010) 182-189.
- [51] C. Bătiu, I. Panea, L. Ghizdavu, L. David, S. Pellascio, *J. Therm. Anal. Calorim.* 79 (2005) 129-134.
- [52] M.A. Diab, A.Z. El-Sonbati, D.M.D. Bader, *Spectrochim. Acta A* 79 (2011) 1057-1062.
- [53] I.S. Yahia, M.S. Abd El-sadek, F. Yakuphanoglu, *Dyes and Pigments* 93 (2012) 1434-1440.

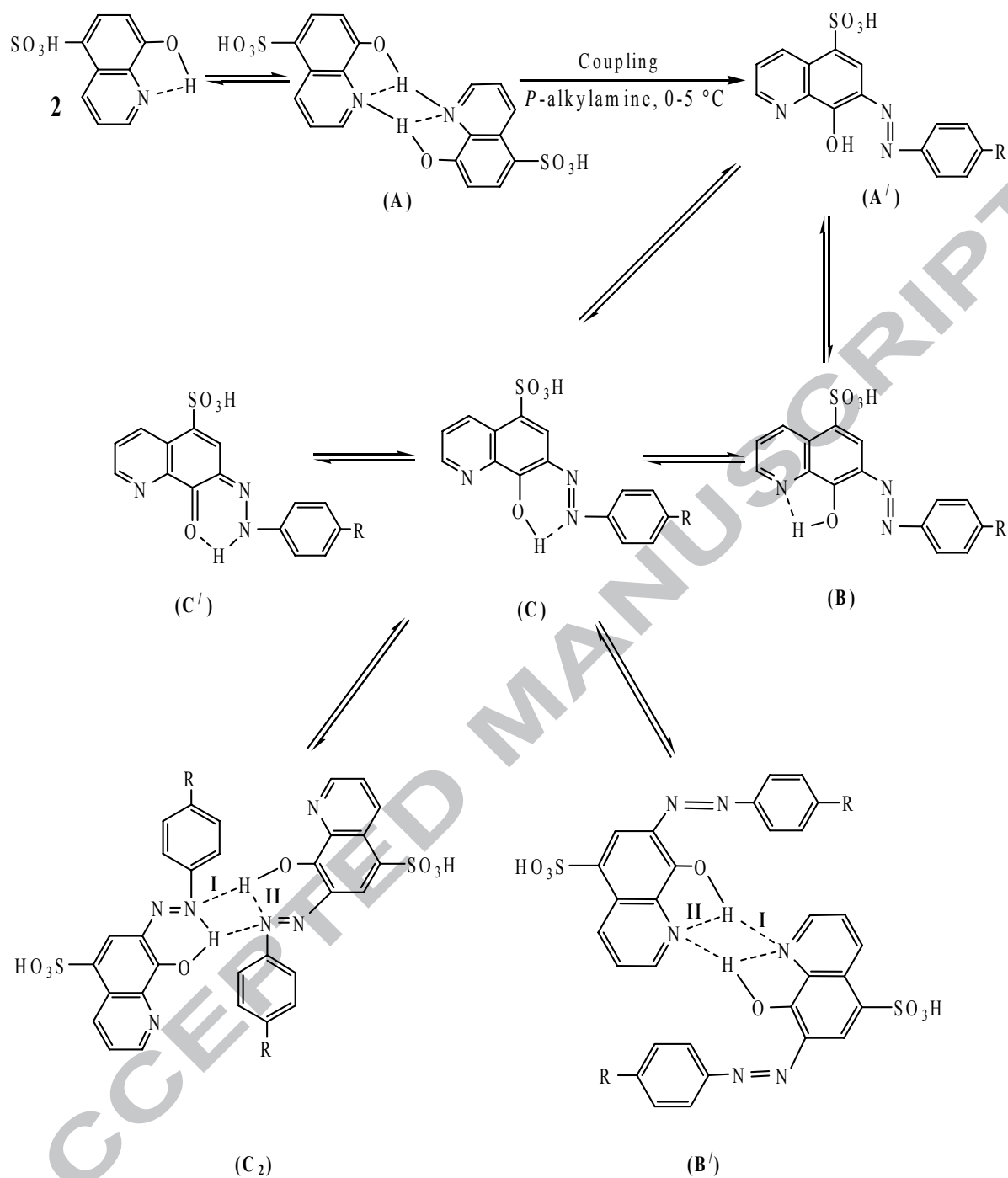


Fig. 1. Representation of the dimeric structure and intramolecular hydrogen bond.

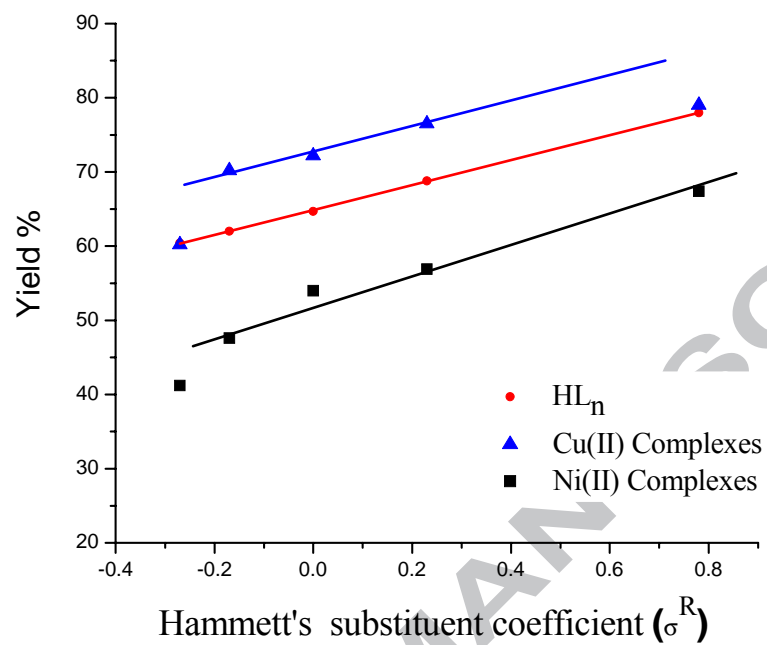


Fig. 2. The relation between Hammett's substituent coefficient (σ^R) and yield %.

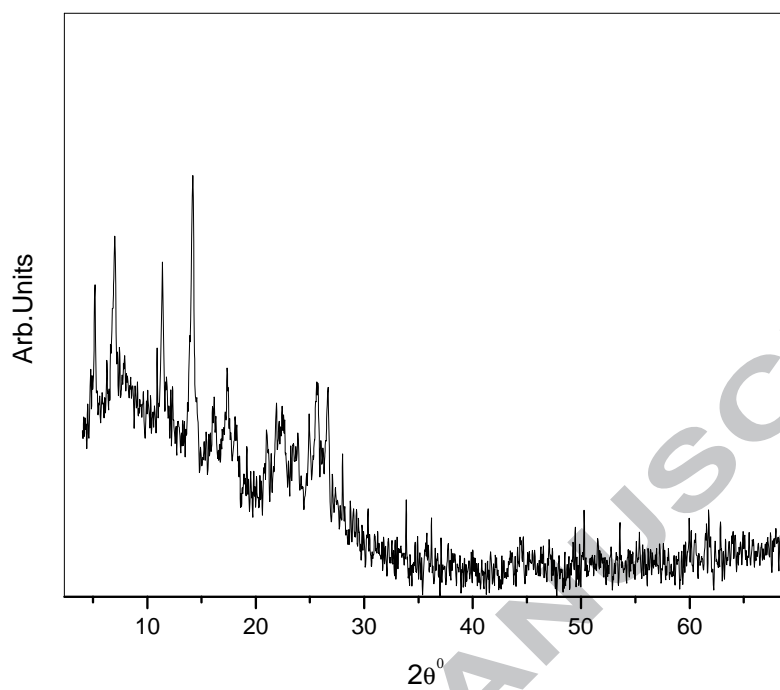


Fig. 3. XRD patterns for [Cu(L₅)₂]

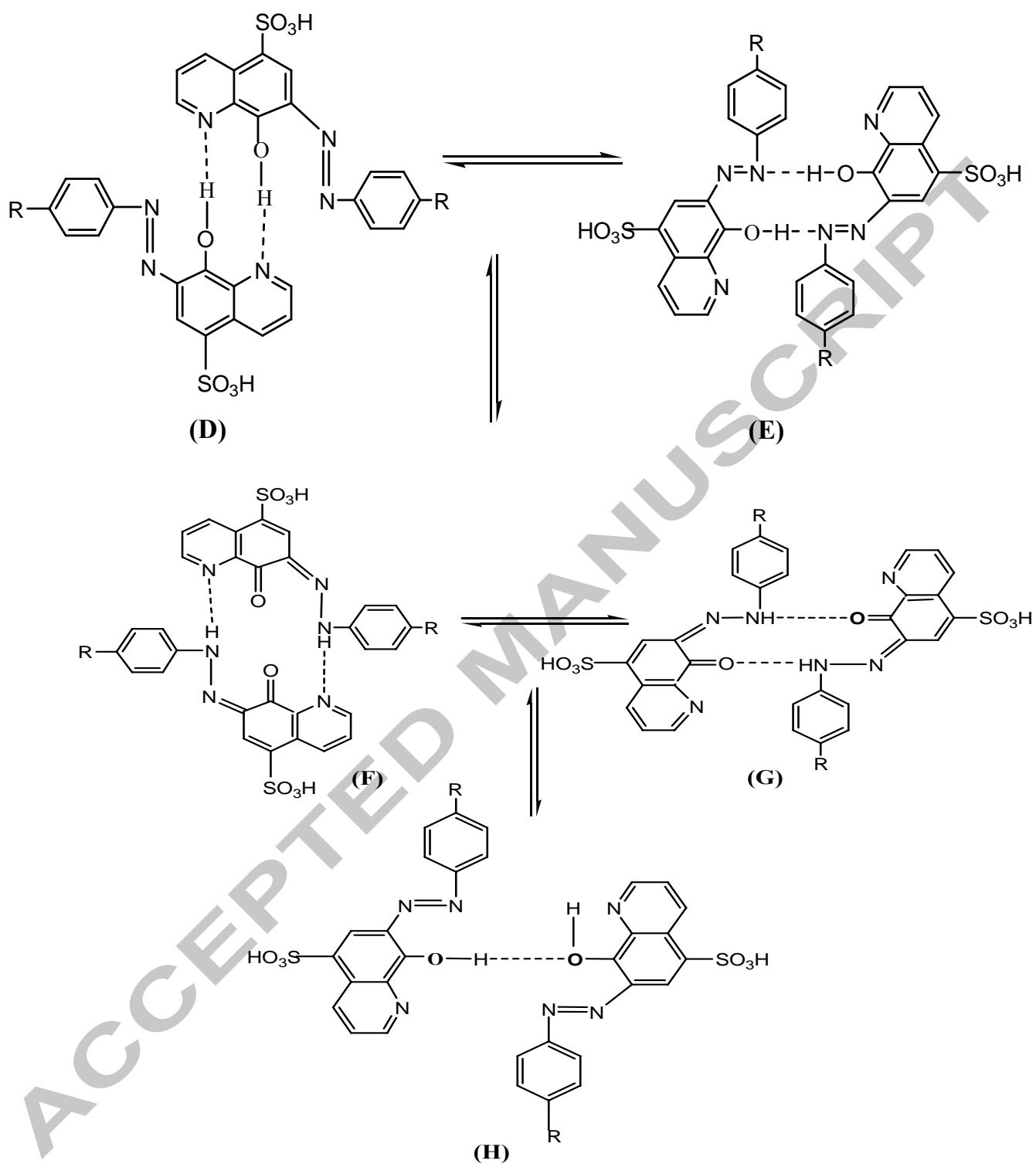


Fig. 4. Intermolecular hydrogen bond.

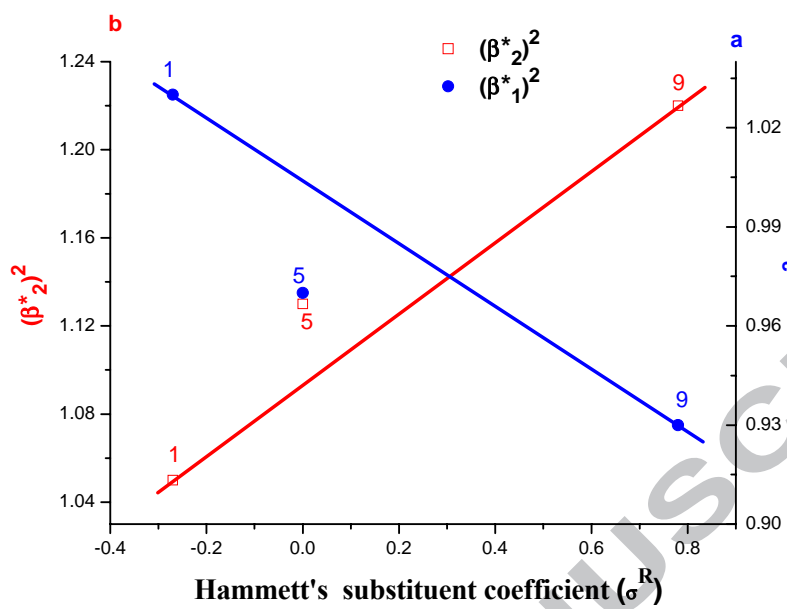


Fig. 5. The relation between Hammett's substituent coefficient (σ^R) vs. a) $(\beta^*_1)^2$ and b) $(\beta^*_2)^2$

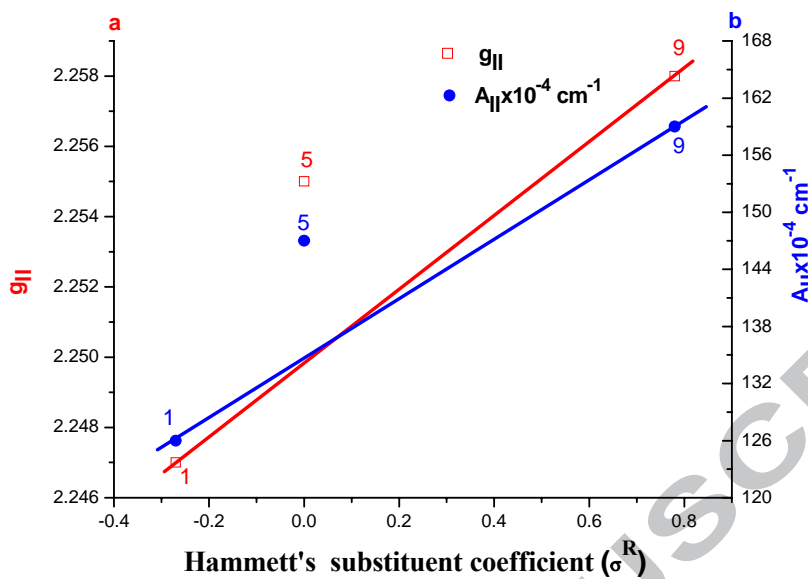


Fig. 6. The relation between Hammett's substituent coefficient (σ^R) vs. a) g_{II} and b) $A_{II} \times 10^{-4} \text{ cm}^{-1}$

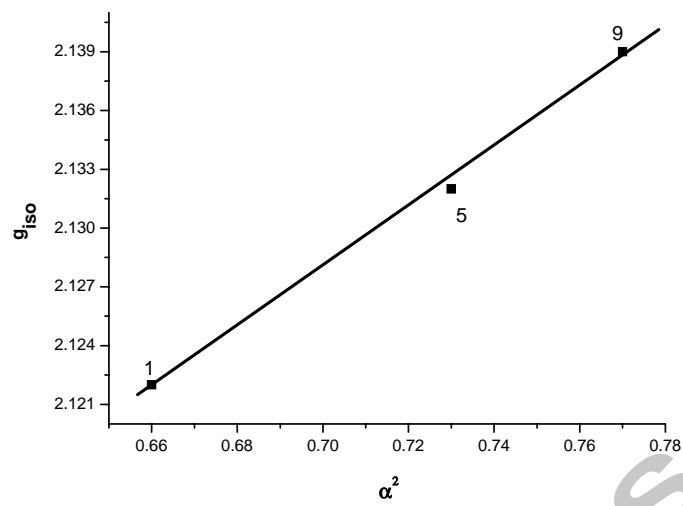
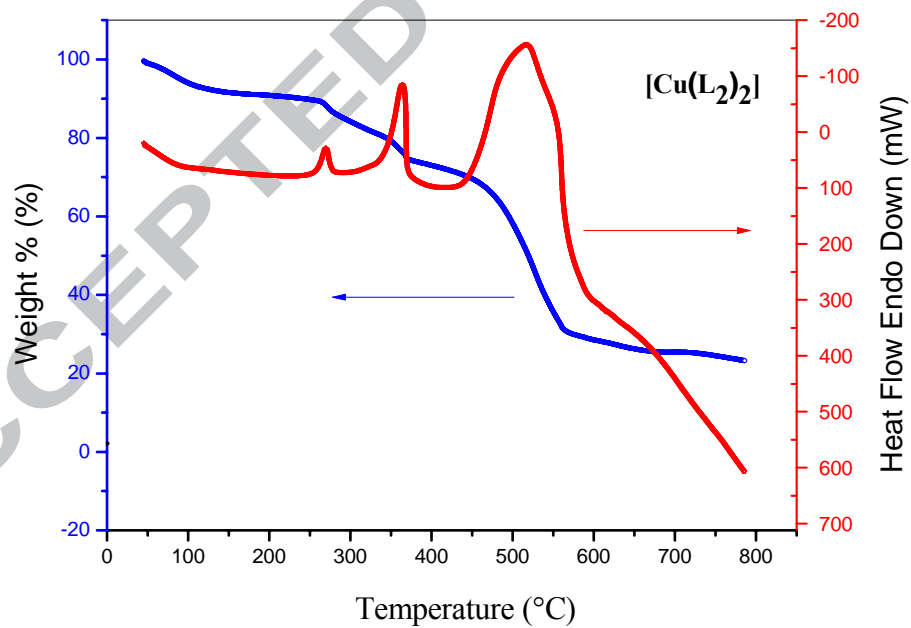
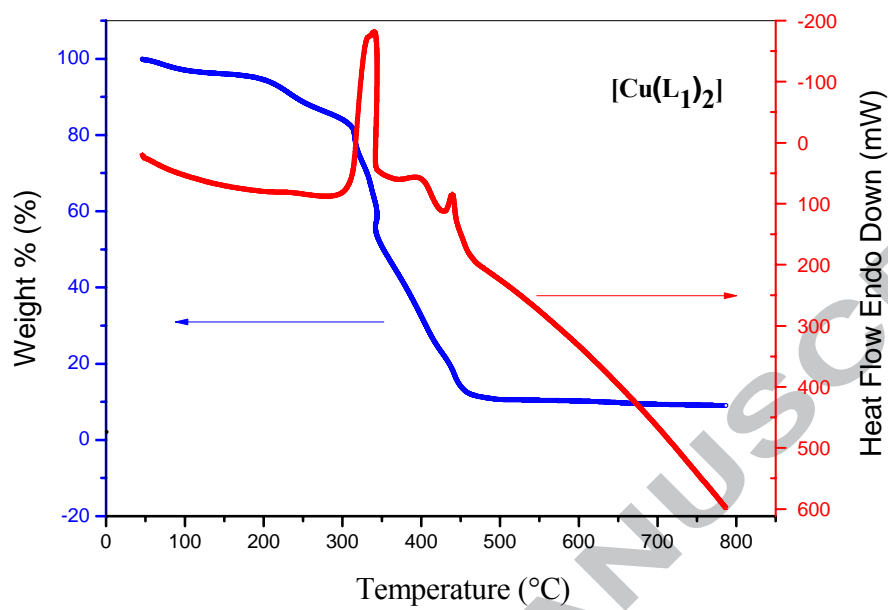
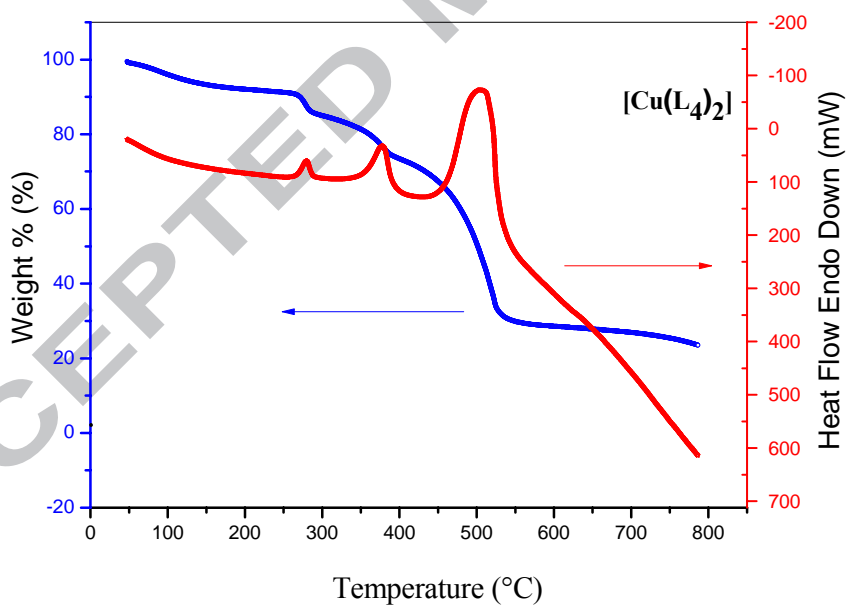
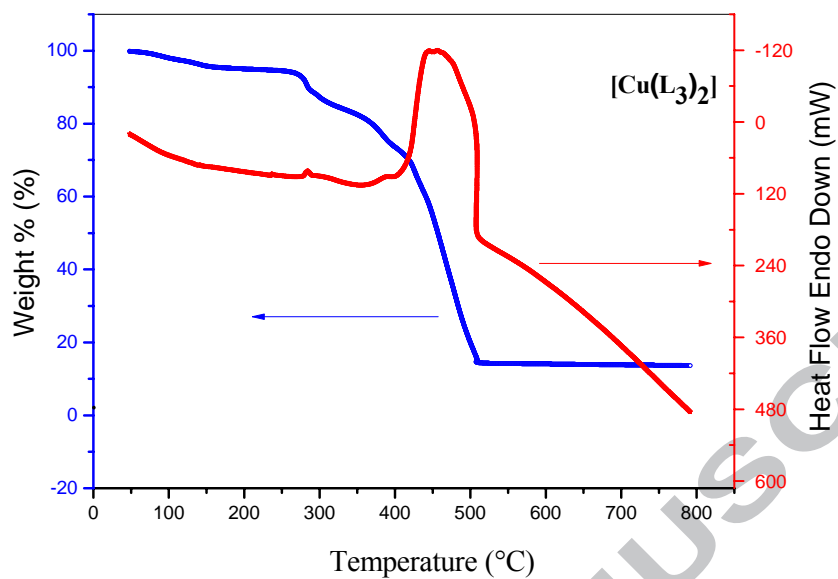


Fig. 7. The relation between g_{iso} vs. α^2





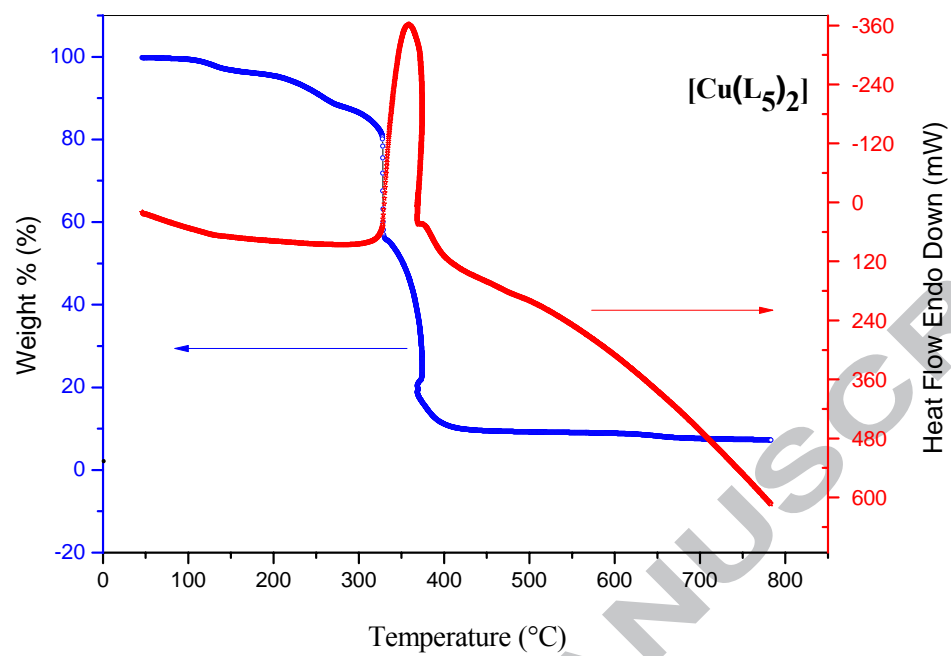


Fig. 8. TGA and DSC curves of the copper(II) complexes

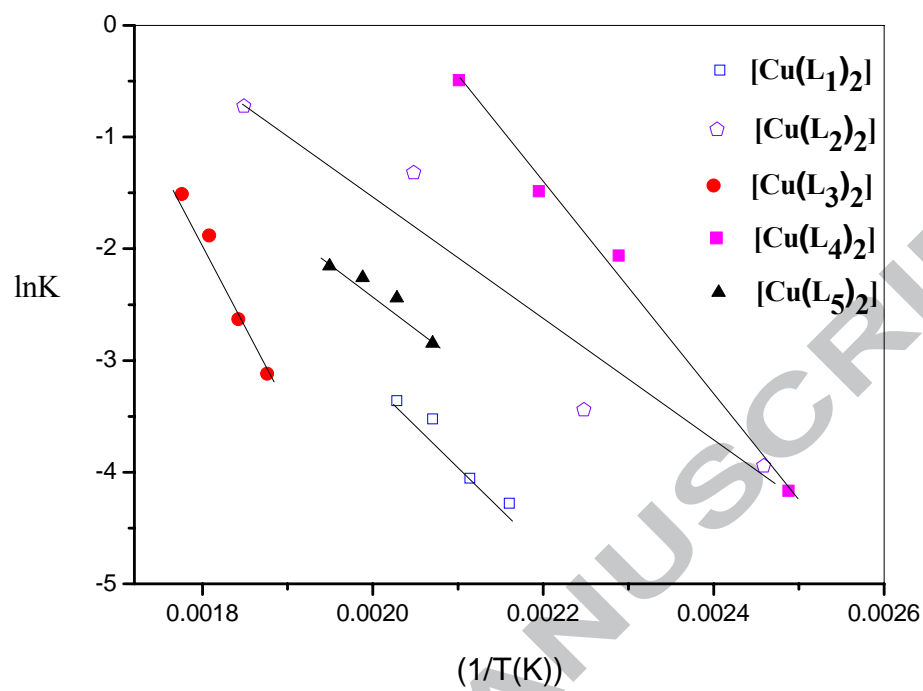
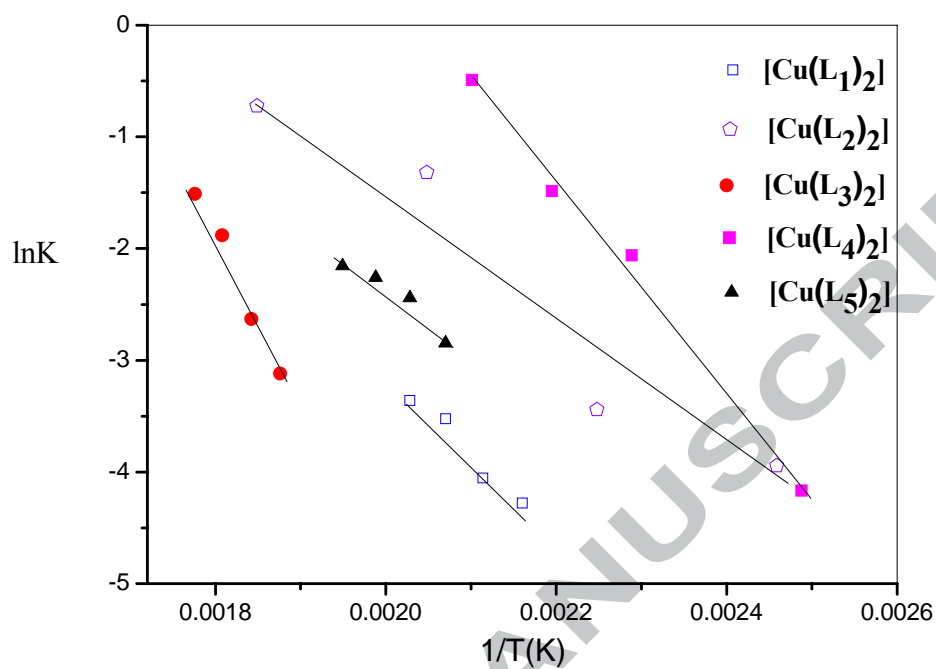


Fig. 9. The relation between $\ln K$ and $1/T$ for copper(II) complexes

The relation between $\ln K$ and $1/T$ for copper(II) complexes



Highlightss

Novel bidentate azodye quinoline ligands were synthesized and characterized.

IR spectra show that the azo compounds (HL_n) act as monobasic bidentate ligand.

All complexes possessed an octahedral and square planar geometry.

The thermal properties of the complexes were investigated using TGA and DSC.

It is found that the change of substituent affects the thermal properties of complexes.

ACCEPTED MANUSCRIPT